

## EVALUATION OF NOTCHED FATIGUE STRENGTH OF OXIDE DISPERSION STRENGTHENING COPPER ALLOY

N. Kawagoishi', Q. Chen', K. Shimana', H. Nisitani<sup>2</sup>, M. Goto', and E. Kondo'

<sup>1</sup> Faculty of Engineering, Kagoshima University, Kagoshima 890-0065, Japan

<sup>2</sup> Faculty of Engineering, Kyushu Sangyo University, Fukuoka 813-8503, Japan

<sup>3</sup> Faculty of Engineering, Oita University, Oita 870-1124, Japan

### ABSTRACT

Rotating bending fatigue tests were carried out at room temperature in air for an aluminum oxide dispersion strengthening copper alloy. The notch sensitivity of the alloy was investigated by using V-grooved specimens and the fatigue strength of notched specimens was evaluated on the basis of linear notch mechanics. The fatigue limits for crack propagation decreases with decrease in notch radius and the notch sensitivity for crack initiation is high. The results were discussed from the characteristics of crack initiation and propagation in the alloy.

### INTRODUCTION

Oxide dispersion strengthening copper alloys are attractive alloys which have found many applications in the modern industries such as the critical components of fusion power generators and wiring harness for automobiles and are expected to be used at higher temperatures due to their high static strength at elevated temperature as well as their excellent electrical and thermal conductivity [1]. It was found in our previous study [2] that strengthening by aluminum oxide dispersion increases the high cycle fatigue strength in these alloys. However, information [3,4] on the fatigue strength of these alloys has

rarely been reported though it is vital for the practical applications. Meanwhile, most machines have complicated structures and there are numerous stress raisers like notches and/or fillets in these structures, which can induce local yielding, lead to the initiation of microcracks and reduce the fatigue strength enormously. Therefore, evaluation of the degradation of fatigue strength due to stress concentration or notch sensitivity is of great importance in practice.

The objective of present study is to investigate the notch sensitivity of an aluminum oxide dispersion strengthening copper alloy under rotating bending loading at room temperature based on the linear notch mechanics [5].

### MATERIAL AND EXPERIMENTAL PROCEDURES

The material used was a round bar (19 mm in diameter) of an aluminum oxide dispersion strengthening copper alloy, GridCop (trademark of SCM Co. Ltd, USA, mentioned as ODSC hereinafter), whose chemical composition (**wt.%**) is 0.26Al, 0.002Fe, 0.0006Pb, 0.016B, and remainder Cu. The alloy was annealed at 1000°C for 1 h and then machined into specimens as shown in Figure 1. The 0.2% proof stress and ultimate strength of the alloy are 366 MPa and 1220 MPa, respectively.

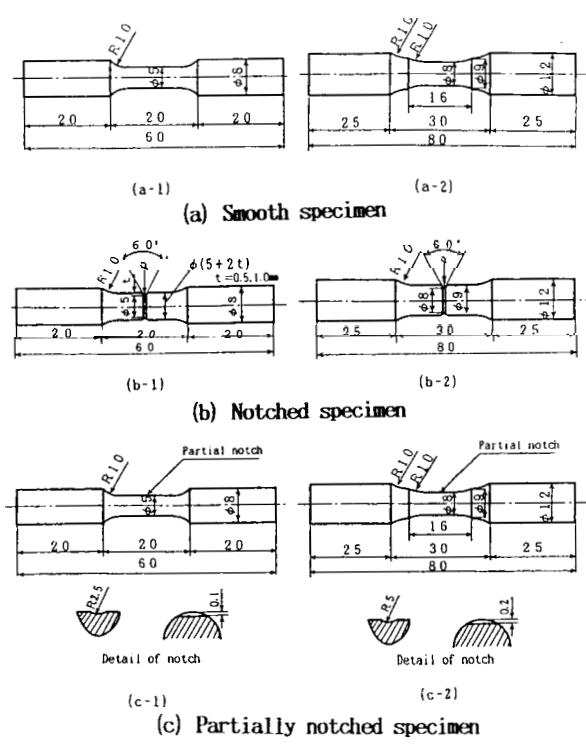


**Figure 1:** Shape and dimensions of (a) smooth, (b) notched, and (c) partially notched specimens

Prior to tests, all the specimens were electro-polished to remove surface layer by  $-20\text{ }\mu\text{m}$  for smooth and partially notched specimens (Figure 1a, 1c), and  $-10\text{ }\mu\text{m}$  for notched specimens (Figure 1b), respectively. The partially notched specimens were used to simulate the fatigue behavior of a small crack in smooth ones (the strength reduction factor  $K_f$  was  $-1.03$ ). Observation of fatigue damage and measurement of crack length were conducted directly under a scanning electron microscope (SEM) or under an optical microscope by using the plastic replica technique. The stress value referred to is the nominal stress amplitude,  $\sigma$ , at net area by ignoring the existence of the notches. Fatigue limit is designated as the limiting stress of non-fracture of a specimen after  $10^7$  cycles of stress repetitions. The tests were carried out at room temperature in air by using Ono-type rotating bending fatigue testing machines with a capacity of  $15\text{ Nm}$ , operating at about  $50\text{ Hz}$  for small specimens (net area diameter  $d = 5\text{ mm}$ ) and  $100\text{ Nm}$ ,  $55\text{ Hz}$  for large specimens ( $d = 8\text{ mm}$ ).

### EXPERIMENTAL RESULTS AND DISCUSSION

Figure 2 shows the S-N curves of smooth and some notched (notch radius  $\rho = 0.05\text{ mm}$ , notch depth  $t = 0.5\text{ mm}$ ) specimens. Figure 3 shows surface states of the partially notched and notched (notch radius  $\rho = 0.05\text{ mm}$ , notch depth  $t = 0.5\text{ mm}$ ) specimens after fatigued for  $10^7$  cycles at fatigue limit. Neither slip bands nor cracks were observed on the whole partial notch area (Figure 3a), meaning that the fatigue limit of a partially notched specimen is determined by the limiting stress for crack initiation. In the case of the notched specimen, however, non-propagating cracks were observed all around the notch root (Figure 3b), signifying that the fatigue limit of a notched specimen is determined by limiting stress for crack propagation.

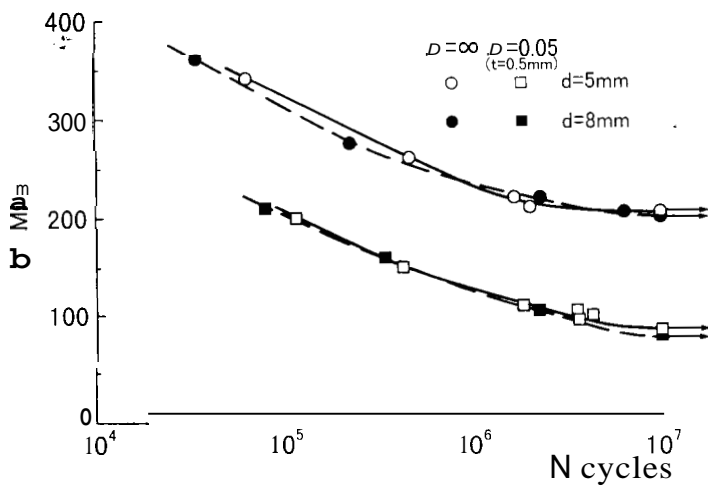


Figure 2: S-N curves

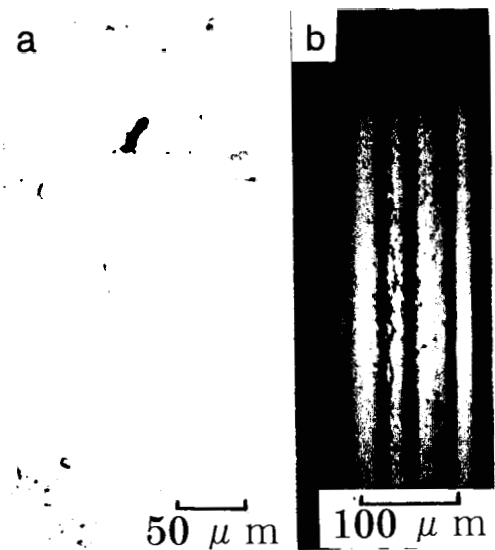


Figure 3: Surface states of (a) partially notched and (b) notched specimens at fatigue limit

Therefore, in the present study, the fatigue limit of a smooth specimen is designated as the fatigue limit for crack initiation,  $\sigma_{w0}$ , while the fatigue limit of a notched specimen is distinguished as the fatigue limit for crack initiation,  $\sigma_{w1}$ , and that for crack propagation,  $\sigma_{w2}$ .

The fatigue results are shown in Table 1. The stress concentration factor,  $K_t$ , is calculated by the body force method [6]. Figure 4 shows the relations between fatigue limits and  $K_t$ . It was reported in many metals that  $\sigma_{w2}$  remains almost unchanged with varying notch radius [7]. However, in the case of ODSC,  $\sigma_{w2}$  reduces with decrease in notch radius or increase in  $K_t$ . To estimate notched fatigue strength under small-scale yielding conditions, Nisitani [5] proposed linear notch mechanics (LNM) based upon the similarity of elastic-plastic fields generated near the notch roots of same notch radius in different specimens subjected to same elastic maximum stress, i.e.  $\sigma_{max} = K_t \sigma_a$ . Although the fatigue limit of a larger smooth specimen was slightly lower than that of a smaller one due to size effect, as shown in Figure 2 and Table 1, this effect was too little and can be neglected.

**TABLE 1: RESULTS OF FATIGUE TESTS**

d (mm)	t (mm)	$\rho$ (mm)	$K_t$	$\sigma_{w1}$ (MPa)	$\sigma_{w2}$ (MPa)	$K_t \sigma_{w1}$ (MPa)	$K_t \sigma_{w2}$ (MPa)	
5	-	$\infty$	1	205	-	205	-	
	0.5	5.0	1.14	185	-	211	-	
		2.5	1.25	185	-	231	-	
		1.0	1.59	150	-	239	-	
		0.3	2.39	115	125	275	299	
		0.1	3.80	75	105	285	399	
		0.05	5.19	60	85	311	441	
	1.0	1.0	1.61	150	-	242	-	
		0.3	2.49	110	120	274	299	
		0.1	4.04	70	100	283	404	
		0.05	5.56	55	75	306	417	
	8	-	$\infty$	1	200	-	200	-
		0.5	1.0	1.81	130	-	235	-
			0.3	2.74	100	110	274	301
0.1			4.16	70	95	291	395	
0.05			5.67	55	80	312	454	

In Figure 5, the maximum elastic stresses  $K_t \sigma_{w1}$  and  $K_t \sigma_{w2}$  at notch root of notched specimens stressed at fatigue limits  $\sigma_{w1}$  ( $\sigma_{w0}$ ) and  $\sigma_{w2}$  are correlated with the reciprocal of notch radius respectively, based on LNM. Each relation can be approximated by a single curve and is independent of the notch depth and net area diameter. This again verifies the validity of LNM in the evaluation of notched fatigue strength of ODSC. The relations in Figure 5 can then be used as master curves to estimate fatigue limits for any specimens with known  $K_t$  and  $\rho$  values.

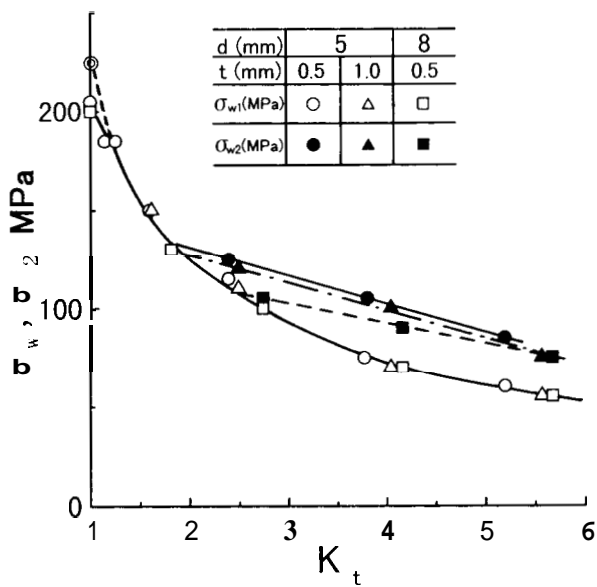


Figure 4:  $\sigma_{w0}$ ,  $\sigma_{w1}$ , and  $\sigma_{w2}$  versus  $K_t$

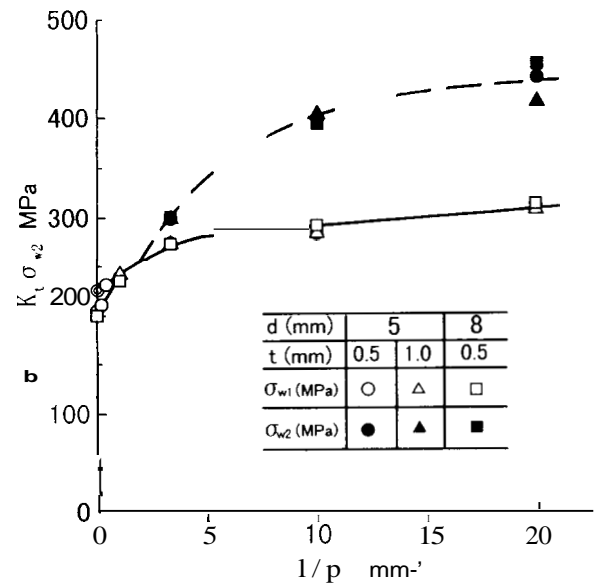


Figure 5:  $K_t \sigma_{w1}$  and  $K_t \sigma_{w2}$  versus  $1/\rho$

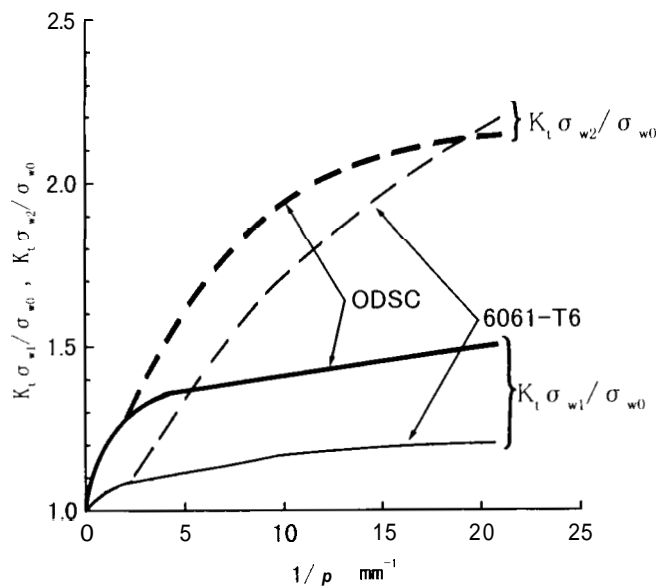
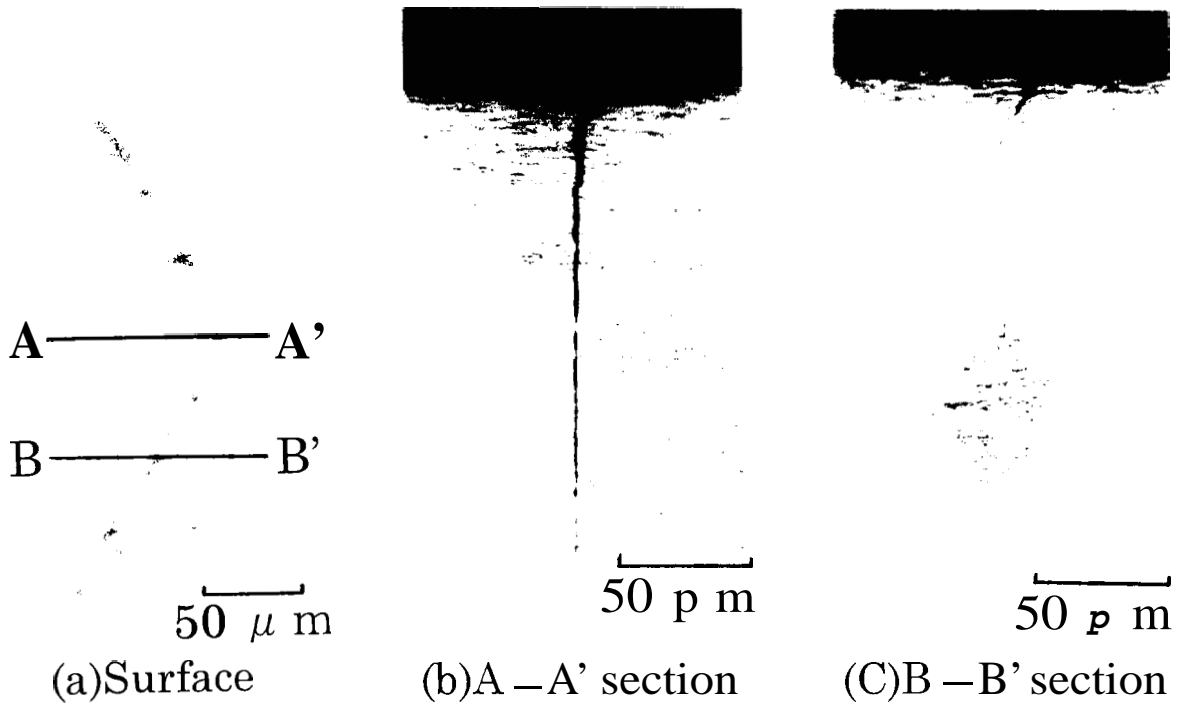


Figure 6:  $K_t \sigma_{w1} / \sigma_{w0}$  and  $K_t \sigma_{w2} / \sigma_{w0}$  versus  $1/\rho$

In Figure 6, the notch sensitivity of ODSC is evaluated on LNM and compared with that of an aged Al alloy **A6061-T6** that was known to be notch sensitive to crack initiation but notch insensitive to crack propagation [S]. The maximum elastic stresses  $K_t \sigma_{w1}$  and  $K_t \sigma_{w2}$  are normalized by the fatigue limit of smooth specimen  $\sigma_{w0}$ . The smaller the ratios of  $K_t \sigma_{w1} / \sigma_{w0}$  and  $K_t \sigma_{w2} / \sigma_{w0}$ , the more sensitive is a material. It is clear that ODSC is relatively notch insensitive to both crack initiation and crack propagation.

Figure 7 illustrates the surface and inner directional propagation morphologies of a crack and Figure 8 shows a SEM micrograph of fracture surface in the partially notched specimens, respectively. As seen from Figures 7-8, a crack in ODSC propagates microscopically in a zigzag manner but macroscopically it grows slightly away from the tensile stress direction, leading to the formation of a quite different fracture morphology from the usually reported semi-elliptically extending pattern.



**Figure 7:** (a) Surface, and (b) and (c) cross sectional morphologies of a crack in partially notched specimen ( $d = 8$  mm,  $\sigma_a = 300$  MPa,  $N = 2.35 \times 10^5$  cycles)

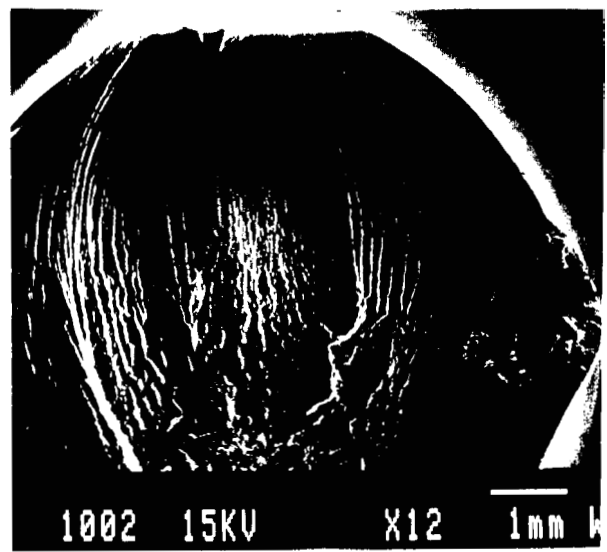
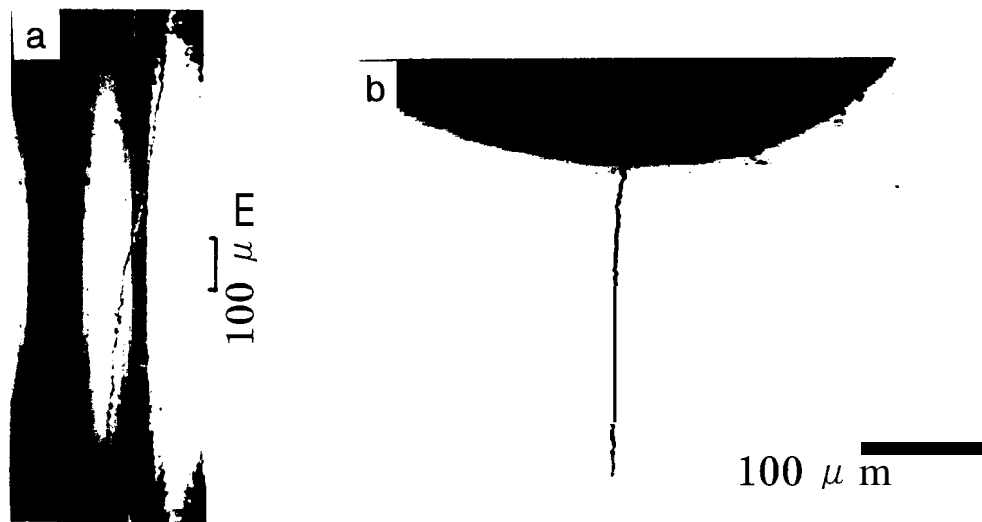


**Figure 8:** Fracture surface of partially notched specimen ( $d = 8$  mm,  $\sigma_a = 300$  MPa)

Figure 9 shows a non-propagating crack observed on notch root and cross section after  $10^7$  cycles of stress repetitions at fatigue limit, respectively. In the case of bluntly notched specimens, a crack is more likely to propagate into large section. However, stress intensity is greater at a sharper notch root and the section area around the notch root increases more rapidly, consequently, crack propagation is easy to be constrained around notch root (Figure 3b). This explains why  $\sigma_{w2}$  decreases with decrease in notch radius and may be related to the anisotropy formed during the severe rolling process of ODSC because the affinity of alumina for copper is small.



Axial direction

**Figure 9:** Non-propagating crack in a notched specimen ( $d = 8$  mm,  $t = 0.5$  mm,  $p = 0.3$  mm) at fatigue limit ( $\sigma_{w2} = 110$  MPa) viewed on (a) notch root and (b) cross section

It was known [2] that crack initiation in ODSC is caused by the sub-micro order surface voids induced in the manufacturing process and the notch sensitivity to crack initiation is high. In other words, the crack initiation in ODSC is nearly determined by the maximum elastic stress at notch root and the effect of stress distribution on crack initiation is small. Therefore, the reason for the larger value of  $K_t \sigma_{w1} / \sigma_{w0}$  in ODSC than in 6061-T6 (Figure 6), lies in that the decrease in fatigue limit of smooth specimen ( $\sigma_{w0}$ ) due to surface voids induced crack initiation was greater than that in fatigue limit for crack initiation ( $\sigma_{w1}$ ) because the probability of voids induced crack initiation is much higher in smooth specimen than in notched ones by statistics [9]. On the other hand, the greater value of  $K_t \sigma_{w2} / \sigma_{w0}$  in ODSC can be explained as a result of that the fatigue limit for crack propagation ( $\sigma_{w2}$ ) is hardly influenced by voids [10].

## CONCLUSIONS

1. Both the fatigue limit for crack initiation and the fatigue limit for crack propagation in notched specimens can be evaluated by linear notch mechanics, respectively.
2. The fatigue limit for crack initiation is notch sensitive, because a crack initiated from small surface voids. That is, the crack initiation related zone is so narrow that the crack initiation is mainly controlled by the maximum stress.
3. The fatigue limit for crack propagation decreases with decrease in notch radius because a crack tends to grow away from tension stress direction and turns into large section area.

## REFERENCES

1. Troxell, J.D. (1995). *Advanced Materials and Processes*, 6/95, 35.
2. Kawagoishi, N., Fujimaki, H., Nisitani, H., Shimana, K., and Ozono, Y. (1998). *Trans. Japan Soc.  $\sigma$  Mech. Eng.* 64A (617), 44.
3. Srivatsan, T.S. and Anand, S. (1993). *Eng. Fract. Mech.* 46 (2), 183.
4. Broyles, S.E., Anderson, K.R., Groza, J.R., and Gilbeling, J.C. (1996). *Met. Mater. Trans. A*, 27, 1217.
5. Nisitani, N. (1983). *Trans. Japan Soc.  $\sigma$  Mech. Eng.* 49A (447), 1353.
6. Nisitani, N. and Noda, N. (1984). *Eng. Fract. Mech.* 20 (5), 743.
7. Kawagoishi, N., Nisitani, H. and Thuno, T. (1990) *Trans. Japan Soc.  $\sigma$  Mech. Eng.* 56A (521), 10.
8. Nisitani, H. and Goto, T. (1976). *Trans. Japan Soc.  $\sigma$  Mech. Eng.* 42A (361), 2666.
9. Takeno, T. (1998). and Nisitani, H. *Trans. Japan Soc.  $\sigma$  Mech. Eng.* 64A (628), 3058.
10. Kawano, T. and Nisitani, H. (1974). *Trans. Japan Soc.  $\sigma$  Mech. Eng.* 40A (333), 1255.